

MedChemComm

Accepted Manuscript



This article can be cited before page numbers have been issued, to do this please use: J. Duan, H. Liu, P. Jeyakkumar, G. Lavanya, S. Li, R. Geng and C. Zhou, *Med. Chem. Commun.*, 2017, DOI: 10.1039/C6MD00688D.



This is an Accepted Manuscript, which has been through the Royal Society of Chemistry peer review process and has been accepted for publication.

Accepted Manuscripts are published online shortly after acceptance, before technical editing, formatting and proof reading. Using this free service, authors can make their results available to the community, in citable form, before we publish the edited article. We will replace this Accepted Manuscript with the edited and formatted Advance Article as soon as it is available.

You can find more information about Accepted Manuscripts in the [author guidelines](#).

Please note that technical editing may introduce minor changes to the text and/or graphics, which may alter content. The journal's standard [Terms & Conditions](#) and the ethical guidelines, outlined in our [author and reviewer resource centre](#), still apply. In no event shall the Royal Society of Chemistry be held responsible for any errors or omissions in this Accepted Manuscript or any consequences arising from the use of any information it contains.



ARTICLE

Design, synthesis and biological evaluation of novel Schiff base-bridged tetrahydroprotoberberine triazoles as new type of potential antimicrobial agents†‡

Received 00th January 20xx,
Accepted 00th January 20xx

DOI: 10.1039/x0xx00000x

www.rsc.org/medchemcomm

Jun-Rong Duan,^a Han-Bo Liu,^a Ponmani Jeyakkumar,^{§a} Lavanya Gopala,^{#a} Shuo Li,^{*b} Rong-Xia Geng^a and Cheng-He Zhou^{*a}

A series of novel Schiff base-bridged tetrahydroprotoberberine (THPB) triazoles were designed, synthesized and characterized for the first time. Antimicrobial assay showed that some of the prepared compounds exerted stronger antibacterial and antifungal activities than the reference drugs. Especially, THPB triazole **7a** gave low MIC values of 0.5, 1 and 2 µg/mL against *B. yeast*, *M. luteus* and MRSA, respectively. Further experiments indicated that the highly active molecule **7a** was able to rapidly kill the MRSA strain and did not trigger the development of bacterial resistance even after 14 passages. The preliminary exploration for antimicrobial mechanism revealed that compound **7a** could effectively intercalate into calf thymus DNA to form **7a**-DNA supramolecular complex, and its Zn²⁺ complex had ability to directly cleave pUC19 DNA, which suggested that compound **7a** might be a potentially dual-targeting antibacterial molecule. It was also found that compound **7a** could be efficiently stored and carried by human serum albumin (HSA), and the hydrophobic interactions and hydrogen bonds played important roles in the transportation of HSA to the active molecule **7a**.

1. Introduction

The increasing resistance of clinical drugs especially currently antimicrobial agents is triggering high morbidity and mortality, which has become one of the most critical health concerns worldwide.¹ Currently, an urgent global task is to combat drug resistance, and it has been universally recognized that no action today means no cure tomorrow. The developments of structurally novel molecules with distinct action mechanisms from the well-known class of antimicrobial agents are therefore of great importance to medical community.²

Berberine has been commonly used in clinic with long history of more than 2000 years in traditional Chinese herbs to treat intestinal infections such as acute gastroenteritis, bacillary dysentery and cholera.³ The unique structure of berberine with a quaternary nitrogen and large desirable π -conjugated backbone enables berberine-based derivatives to readily bind with biomolecules like deoxyribonucleic acid (DNA) or enzyme via noncovalent forces such as π - π stacking and

electronic interactions, thus exerting potent biological activities. Notably, despite of its long term clinical use, the incidence of resistance of berberine is less reported.⁴ This attracts special interest in investigating berberines for possible further antimicrobial use and other medicinal potentiality like anticancer, antiviral, antiinflammatory, antiparasitic activities etc.⁵ However, berberine exhibits poor solubility, low bioavailability *in vivo* and some of the severe side effects such as anaphylactic shock and drug eruption, and these have seriously limited its useful profile. Therefore much effort has been devoting towards the structural modification of berberine. Literature revealed that structural changes such as disruption of symmetry or molecular planarity were proved to be an effective way to improve the intrinsic water solubility.⁶ Tetrahydroprotoberberine (THPB) was found to be good structural alternative with large medicinal potentiality.⁷ An increasing exploitation is directing towards THPBs for their medicinal value, especially in anti-infective aspects.⁸

Azole compounds are well known types of heterocycles with various bioactivities, have been extensively designed and synthesized as antimicrobial drugs.⁹ Particularly triazole nucleus is a poly-nitrogen electron-rich heterocycle present in many biologically active compounds. It is generally considered that triazole fragment is stable to metabolic degradation and capable of forming hydrogen bonds, thus the introduction of triazole nucleus is beneficial to improve the binding with biomolecular targets and increase water solubility of target compounds.¹⁰ Therefore triazole moiety is prevalently employed in drug design, so far a large number of predominant triazole-based medicinal drugs have been successfully

^a Institute of Bioorganic & Medicinal Chemistry, Key Laboratory of Applied Chemistry of Chongqing Municipality, School of Chemistry and Chemical Engineering, Southwest University, Chongqing 400715, PR China. E-mail: zhouch@swu.edu.cn; Fax: +86 23 68254967; Tel: +86 23 68254967

^b School of Chemical Engineering, Chongqing University of Technology, Chongqing 400054, PR China. E-mail: lishuo@cqut.edu.cn

† The authors declare no competing interests.

‡ Electronic supplementary information (ESI) available. See DOI: 10.1039/x0xx00000x

§ Ph.D candidate from India.

Postdoctoral fellow from Sri Venkateswara University, Tirupati 517502, India.

developed and prevalently used in clinic, especially in antimicrobial aspect, such as fluconazole, itraconazole, voriconazole, posaconazole, efinaconazole and terconazole

etc.¹¹ Their importantly clinical uses have been motivating extensive efforts to construct new bioactive molecules based on triazole fragment.

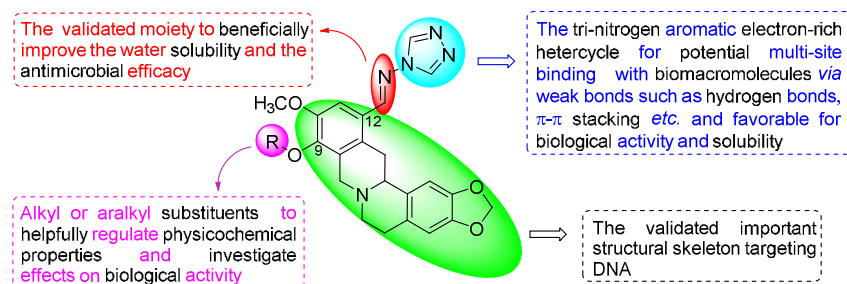
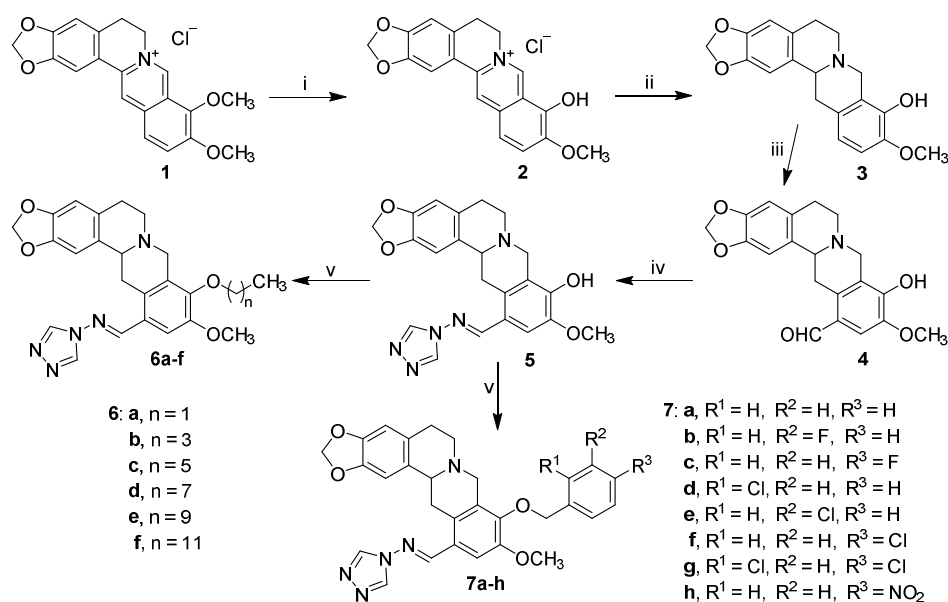


Fig. 1 Design of novel Schiff base-bridged tetrahydropberberine triazoles.

Our previous work showed that the introduction of azoles such as imidazole, triazole and benzimidazole moieties into the C-9 or C-12 position of berberine backbone was not only beneficial to enhance the antimicrobial activities but also widen the antimicrobial spectrum, including against methicillin-resistant *Staphylococcus aureus* (MRSA).¹² However, to our best knowledge, the combination of azoles and THPB backbone has been rarely reported. In view of above consideration and as an extension of our ongoing research on bioactive heterocycles, it is of great interest for us to combine THPB with triazole nucleus to generate a new structural type of potentially antimicrobial agents via Schiff base bridge which is a validated moiety to beneficially improve the water solubility and the antimicrobial efficacy (Fig. 1).¹³ It is expected that these hybrids of THPB with triazole moiety could not only beneficially enhance the antimicrobial activities and broaden the antimicrobial spectrum, but also helpfully improve water solubility. Literature revealed that lipophilic substituents on berberine especially at C-9 position could significantly influence the bioactivities by modifying molecular flexibility

and regulating the lipid-water partition coefficient.¹⁴ Rationally, various aliphatic chains with different lengths and substituted benzyl moieties including chloro, fluoro and nitro groups were incorporated into C-9 position of THPB to investigate their effects on antimicrobial activities. The synthetic route of target THPB triazoles was shown in Scheme 1. All the newly synthesized compounds were confirmed by spectral analysis and screened against Gram-positive bacteria including MRSA, Gram-negative bacteria and fungi. Aqueous solubility, bactericidal kinetic assay and antibacterial resistance to the highly active molecule were also investigated. In order to explore the preliminary antimicrobial action mechanism, the interaction of the most active triazole derivative with DNA was further carried out by fluorescence and UV-vis absorption spectroscopy as well as agarose gel electrophoresis. Additionally, the binding behavior of the highly active molecule to human serum albumin (HSA) was investigated to preliminarily study the absorption, distribution, and metabolism.



Scheme 1. Reagents and conditions: (i) berberine, 20 mm Hg, 190 °C, 15 min; CH₃CH₂OH-HCl; (ii) CH₃OH, NaBH₄, rt 4 h; (iii) (a) HMTA/TFA, 120 °C, 3 h; (b) 10% H₂SO₄, 90–100 °C, 2 h; (iv) CH₃CH₂OH, CH₃COOH, reflux, 5 h; (v) alkyl bromides and halobenzyl halides, K₂CO₃, DMF, 80 °C.

2. Chemistry

All the target compounds were conveniently prepared from commercial berberine chloride, 4*H*-1,2,4-triazol-4-amine, alkyl bromides and halobenzyl halides. As depicted in Scheme 1, berberrubine **2** was easily obtained in 84.6% yield by the 9-demethylation of berberine chloride **1** at 190 °C under vacuum,¹⁵ and was further reduced by NaBH₄ to give THPB **3** at 0 °C in 63.1% yield. The formylation of compound **3** by hexamethylenetetramine (HMTA) in trifluoroacetic acid under reflux produced the important intermediate **4** in high yield of 76.5%,¹⁶ which proceeded more facilely and efficiently in comparison to the literature method.¹⁷ The latter was condensed with 4*H*-1,2,4-triazol-4-amine in ethanol under reflux using a catalytic amount of glacial acid to afford the target Schiff base **5** in 88.3% yield. The further structural modification of compound **5** by alkyl or substituted aromatic halides generated the alkyl derivatives **6a–f** and aralkyl ones **7a–h** with the yields from 15.2 to 35.4% in DMF at 80 °C using potassium carbonate as the

base. All the new compounds were confirmed by IR, ¹H NMR, ¹³C NMR and HRMS spectra (ESI†).

3. Results and discussion

3.1 Antimicrobial activities

The obtained results in Table 1 showed that almost all the synthesized THPBs displayed better *in vitro* biological activity than precursor berberine against most of the tested strains. Towards *M. luteus* and *B. typhi*, the intermediate **4** with a formyl group at the 12-position of THPB gave comparable or superior antibacterial efficacy to chloromycin and norfloxacin. Generally, the target THPB triazoles gave better inhibitory potency than precursor berberine and the corresponding intermediate **4**, and some of them were much more active than reference drugs. It revealed that the triazole fragment at the 12-position of THPB should play an important role in exerting antibacterial potency.

Table 1 Antibacterial data as MIC (μg/mL) for compounds **4–7**^{a,b}.

Compds	Gram-positive bacteria				Gram-negative bacteria					
	<i>S. aureus</i>	MRSA	<i>B. subtilis</i>	<i>M. luteus</i>	<i>E. coli</i> JM109	<i>E. coli</i> DH52	<i>S. dysenteriae</i>	<i>P. aeruginosa</i>	<i>B. proteus</i>	<i>B. typhi</i>
4	128	256	32	2	256	256	512	16	64	2
5	64	16	512	1	128	128	256	128	64	128
6a	256	8	128	16	256	512	512	256	32	256
6b	16	8	16	1	16	32	8	16	16	16
6c	8	32	8	16	4	32	8	32	16	2
6d	8	16	16	16	32	16	64	512	16	16
6e	32	32	32	64	128	64	128	128	64	16
6f	256	512	256	512	512	256	512	512	256	256
7a	8	2	32	1	32	16	32	8	16	4
7b	256	512	512	32	>512	256	256	16	64	512
7c	32	8	32	2	32	16	16	8	128	4
7d	16	16	32	256	4	64	16	2	512	1
7e	256	256	512	512	0.5	512	64	512	512	256
7f	8	32	16	16	8	32	64	4	8	8
7g	16	8	32	128	16	256	512	32	32	32
7h	512	16	256	2	128	512	64	64	512	4
Berberine	512	128	>512	>512	–	>512	256	256	–	–
Chloromycin	16	16	32	8	32	32	32	32	32	32
Norfloxacin	0.5	8	4	2	1	1	4	16	8	4

^a Minimal inhibitory concentrations were determined by micro broth dilution method for microdilution plates.

^b *S. aureus*, *Staphylococcus aureus* ATCC25923; MRSA, Methicillin-Resistant *Staphylococcus aureus* N315; *B. subtilis*, *Bacillus subtilis* ATCC6633; *M. luteus*, *Micrococcus luteus* ATCC4698; *E. coli* JM109, *Escherichia coli* JM109; *E. coli* DH52, *Escherichia coli* DH52; *S. dysenteriae*, *Shigella dysenteriae*; *P. aeruginosa*, *Pseudomonas aeruginosa* ATCC27853; *B. proteus*, *Bacillus proteus* ATCC13315; *B. typhi*, *Bacillus typhi*.

The preliminary structure–activity relationships (SARs) demonstrated the significant effect of the substituents at the 9-position of THPB on biological activities. In contrast with the clinical drugs chloromycin and norfloxacin, the unsubstituted compound **5** at the 9-position of THPB nucleus exhibited weaker activity against all the tested strains except for *M. luteus* which was the most sensitive to compound **5** with low MIC value of 1 μg/mL.

In general, most of the alkyl-substituted compounds could effectively inhibit the growth of all the tested bacterial strains *in vitro*. Among the alkyl derivatives **6a–f**, the butyl compound **6b** and the hexyl analogue **6c** gave broader antibacterial spectrum and better activities with MIC values of 1–32 μg/mL.

Noticeably, compound **6b** exhibited the best anti-*M. luteus* activity with a MIC value of 1 μg/mL, which was superior to standard drugs chloromycin (MIC = 8 μg/mL) and norfloxacin (MIC = 2 μg/mL). Towards *E. coli* JM109 and *B. typhi* strains, compound **6c** displayed 8- and 16-fold more potent inhibitory activity (MIC = 4 and 2 μg/mL, respectively) than chloromycin. It also demonstrated effective anti-*S. aureus*, anti-*B. subtilis* and anti-*S. dysenteriae* activities with MIC values of 8 μg/mL, being more potent than chloromycin. Moreover, when the alkyl substituents were extended to decyl and dodecyl groups, compounds **6e** and **6f** showed poor or even no activity against most of the tested bacterial strains. However, the ethyl derivative **6a** was also less beneficial for the antibacterial

ARTICLE

Journal Name

efficiency even at high concentration. These results revealed that either decrease or increase of the alkyl chain length was unfavorable for the bioactivity, and only proper length chain in THPBs exerted an important influence in enhancing bioactivity. The short alkyl chains with poor lipophilicity and long alkyl chains with good lipophilicity in these THPBs might make them unfavorable for being delivered to the binding sites.

In comparison with the alkyl derivatives, most of the aralkyl-substituted ones **7a–h** exerted relatively better activities in inhibiting the growth of the tested strains. Notably, compound **7a** without substitution on phenyl ring gave the best antibacterial efficiencies with MIC values of 1–32 µg/mL towards the corresponding bacteria. It was found that *M. luteus*, MRSA and *P. aeruginosa* were sensitive to THPB triazole **7a** with MIC values of 1, 2 and 8 µg/mL, respectively, which were superior to those of chloramphenicol and norfloxacin. Excitedly, the target compounds **6a**, **6b**, **7a**, **7c** and **7g** exerted good biological activities against MRSA with MIC values of 2–8 µg/mL, which were more active than chloramphenicol (MIC = 16 µg/mL). Especially compound **7a** exhibited 8- and 4-fold more activity towards MRSA with low concentration (MIC = 2 µg/mL) than chloramphenicol and norfloxacin, respectively. These indicated that compound **7a** had the potency to be a lead molecule in the development of more effective antimicrobial agents with broad spectrum. Continual study revealed that the *ortho*- and *para*-substituted benzyl derivatives **7c**, **7d** and **7f** were more effective against most of the tested bacteria than the *meta*-substituted ones **7b** and **7e**. Particularly, 2-chlorobenzyl derivative **7d** gave potent inhibition against *P. aeruginosa* (MIC = 2 µg/mL) and *B. typhi* (MIC = 1 µg/mL), which was more active than chloramphenicol and norfloxacin. Unfortunately, 4-nitrobenzyl compound **7h** displayed relatively poor activity against most of the tested bacteria, which suggested that the introduction of electron withdrawing group like NO₂ might be not helpful for antibacterial activity. Among all the prepared compounds, the 3-chlorobenzyl derivative **7e** gave the strongest activity against *E. coli* JM109 with a MIC value of 0.5 µg/mL, it showed that this compound might be hopeful to be developed as special anti-*E. coli* JM109 agent.

The antifungal evaluation *in vitro* showed no remarkable activities for 12-formyl THPB **4** and 9-unsubstituted THPB triazole **5** against the tested fungi except for *B. yeast* which was highly sensitive to compound **4** (MIC = 1 µg/mL). However, the structural modification at the 9-position of THPB nucleus generated THPB triazole derivatives which displayed potent antifungal activities towards most of the tested fungal strains. It was noticed that the antifungal abilities of the alkyl compounds displayed similarity to their antibacterial efficiencies. The suitable length of alkyl chain seemed to be hexyl chain, the hexyl derivative **6c** exerted the best antifungal efficacy with MIC values ranging from 2 to 32 µg/mL against all the tested fungi, better than other alkyl derivatives with shorter or longer chain length. Among the aralkyl THPB triazoles **7a–h**, the 4-chlorobenzyl derivative **7a** gave more effective antifungal potency with MIC values of 0.5–32 µg/mL than other aralkyl-substituted compounds. Particularly, the same low MIC values of 0.5 µg/mL were observed for THPB triazole **7a** towards *B. yeast*, **7b**

towards *C. albicans* and **7f** towards *C. utilis*, and this suggested that these compounds should be much more active than reference drug fluconazole, and they might have large possibility as new antifungal agents and should be worthy to be investigated deeply (ESI† Table S1).

3.2 Effect of clogP values and aqueous solubility of selected compounds

THPB triazoles **5**, **6b**, **6c**, **6f**, **7a**, **7c** and **7f** were further selected for soluble profile. The water solubility (mg/mL) was evaluated at physiological pH and the obtained results were depicted in Table 2. In general, the THPB triazoles were more soluble in water than berberine. Particularly, the THPB triazole **7f** bearing 4-chlorobenzyl substituent showed the largest water solubility in this series, 7 times higher than berberine. The highly bioactive derivative **7a** possessed equivalent solubility to its fluorinated counterpart **7c** with 2-fold enhanced soluble potency in contrast with berberine. Remarkably, the alkyl derivatives were less soluble in water than benzyl ones. Among the alkylated THPBs **6b**, **6c** and **6f**, the hexyl derivative **6c** was endowed with more potent aqueous solubility, more than five times as soluble as berberine. Unfortunately, the replacement of hexyl group by dodecyl moiety dramatically led to a decrease in solubility. These results indicated that the insertion of triazole moiety in THPB backbone should be beneficial for the improvement of aqueous solubility.

Hydrophobic/lipophilic property played an important role in predicting pharmacokinetic properties of a drug and its interaction with macromolecular targets. The calculated lipid/water partition coefficients (clogP) of some target compounds and berberine were shown in Table 2. The synthesized compounds **6b–c**, **7a**, **7c** and **7f** with moderate clogP values exhibited better antimicrobial activities, indicating that compounds with suitable lipophilicity were favorable to permeate through biological membrane and to be delivered to the binding sites.

Table 2 ClogP values and evaluation of solubility of selected compounds (Mean ± SD, n = 3)^{a,b}.

Compds	ClogP	Aqueous solubility
4	2.99	0.079 ± 0.002
5	0.58	0.392 ± 0.024
6b	2.65	0.121 ± 0.016
6c	3.70	0.442 ± 0.028
6f	6.88	0.097 ± 0.006
7a	2.83	0.178 ± 0.027
7c	2.97	0.185 ± 0.013
7f	3.54	0.613 ± 0.034
Berberine	–	0.085 ± 0.005

^aClogP values were calculated by ChemDraw Ultra 14.0. ^bIn mg/mL, determined in pH 7.4 phosphate buffer, at 30 °C.

3.3 Bactericidal kinetic assay

The ability of an antibacterial agent to rapidly eradicate MRSA would decrease when this agent emerged resistance towards bacteria.¹⁸ To examine the antibacterial potency of the promising compound, a time-kill assay was performed by checking the viability of exponentially growing MRSA against the highly active compound **7a**. As shown in Fig. 2, compound **7a** showed more than 3 log (CFU/mL) reduction in the number of viable bacterial within an hour

at a concentration of $4 \times \text{MIC}$. Fig. 2 indicated a rapidly killing effect for compound **7a** against MRSA.

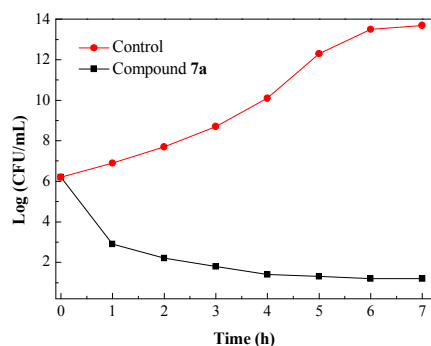


Fig. 2 Time-kill kinetics of compound **7a** ($4 \times \text{MIC}$) against MRSA.

3.4 Resistance study

The emergence of bacterial resistance towards most of the clinical drugs currently is a serious problem, especially MRSA strain towards norfloxacin.¹⁹ Hence, it would be important to evaluate the propensity of THPB triazole **7a** to induce bacterial resistance. This work investigated the ability of susceptible pathogen MRSA to develop resistance against compound **7a**, and norfloxacin was used as a positive control. The standard strain of MRSA was exposed to the increasing concentrations of compound **7a** from MIC for the sustained passages, and the new MIC values were determined against each passage of MRSA. Fig. 3 exhibited no obvious change in the MIC for compound **7a** even after 14 passages, whereas norfloxacin gave significant increase in the MIC after 5 passages against MRSA. The obtained results suggested that MRSA was more

difficult to develop resistance against compound **7a** than the clinical drug norfloxacin.

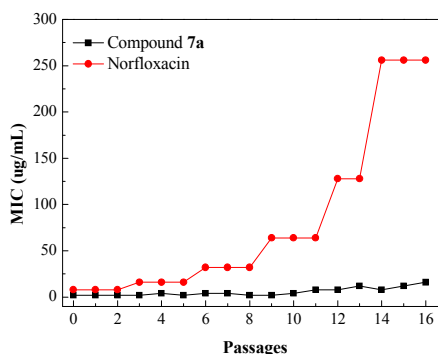


Fig. 3 Evaluation of resistance development against compound **7a** in bacterial strain MRSA.

3.5 Molecular modeling

To rationalize the observed antibacterial activity and investigate the anti-MRSA action mechanism of THPB triazole **7a**, molecular docking study was performed between compound **7a** and MRSA DNA (PDB ID: 2XCS). As shown in Fig. 4, the OCH_2O group of the THPB **7a** was adjacent to the ARG-1122 and MET-1121 residues, forming three hydrogen bonds with a distance of 2.1, 2.4 and 2.9 Å, respectively. Besides, the ARG-1122 and GLY-1072 residues could also form hydrogen bonds with methoxy group of THPB fragment and N atom of triazole ring. The hydrogen bonds might be favorable to stabilize the **7a**-DNA complex, which might be responsible for the good inhibitory efficacy of compound **7a** against MRSA.

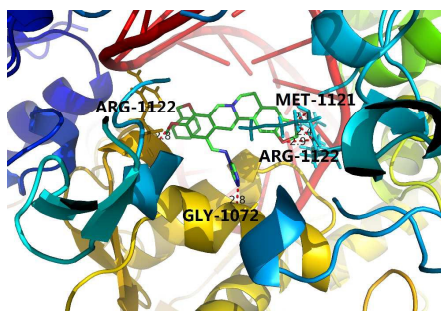
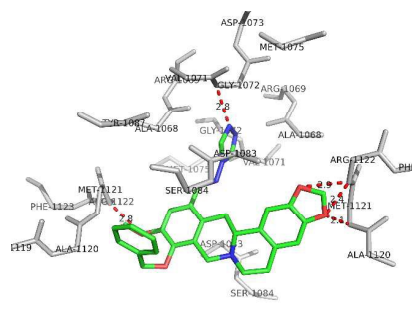


Fig. 4 Molecular modeling of compound **7a** and MRSA DNA.



3.6 Interactions with calf thymus DNA

DNA is the main cellular target for studies with small molecules of biological importance, and as a therapeutic target it has been extensively employed in rational design and construction of new and effective drugs.²⁰ Calf thymus DNA was commonly selected as DNA model due to its medically important, low-cost and ready available properties. To explore the possible mechanism of antimicrobial action, the interaction of the highly active compound **7a** with DNA at molecular level was investigated by UV-vis spectroscopy.

3.6.1 Absorption spectra of DNA in the presence of compound **7a**

In absorption spectroscopy, hyperchromism and hypochromism are perceived as important spectral features to distinguish change of the DNA double-helix structure. As literature reported, hypochromism

indicate a close proximity of the aromatic chromophore to the DNA bases due to the interaction between the electronic states of intercalating chromophore and that of the DNA base.²¹

With a fixed concentration of DNA, UV-vis absorption spectra were recorded with sequentially increasing amount of compound **7a**. As shown in Fig. 5, UV-vis spectra gave a proportional increase at 260 nm for the maximum absorption peak of DNA and a slightly red shift with the increasing concentration of compound **7a**. Meanwhile, the absorption value of simply sum of free DNA and free compound **7a** was a little greater than the measured value of **7a**-DNA complex (inset of Fig. 5). This suggested a hypochromic effect between DNA and compound **7a**. Furthermore, the intercalation of the chromophore fragment of compound **7a** into the DNA helix and the strong overlap of π - π^* states of the large π -conjugated system with

ARTICLE

Journal Name

the electronic states of DNA bases were in accordance with the observed spectral changes.

On the basis of variations in the absorption spectra of DNA upon binding to compound **7a**, the binding constant K can be calculated by the following equation:

$$\frac{A^0}{A - A^0} = \frac{\xi_c}{\xi_{D-C} - \xi_c} + \frac{\xi_c}{\xi_{D-C} - \xi_c} \times \frac{1}{K[Q]} \quad (1)$$

A^0 and A represent the absorbance of DNA in the absence and presence of compound **7a** at 260 nm, ξ_c and ξ_{D-C} are the absorption coefficients of compound **7a** and compound **7a**–DNA complex, respectively. The plot of $A^0/(A - A^0)$ versus $1/[\text{compound } \mathbf{7a}]$ is constructed by using the absorption titration data and linear fitting (ESI†, Fig. S1), yielding the binding constant, $K = 2.27 \times 10^4$ L/mol, ($R = 0.999$, $SD = 0.110$). The experimental results revealed that THPB triazole **7a** possessed a good DNA-binding ability with calf thymus DNA, which was also consistent with the above mentioned hypochromic effect.

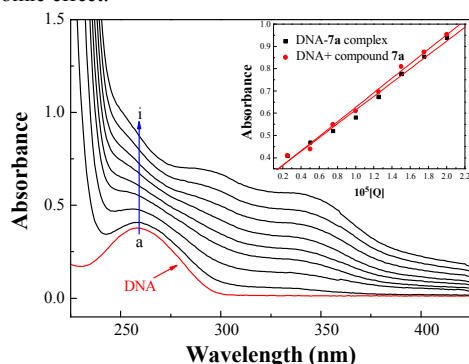


Fig. 5 UV absorption spectra of DNA with different concentrations of compound **7a** (pH = 7.4, $T = 303$ K). Inset: comparison of absorption at 260 nm between the **7a**–DNA complex and the sum values of free DNA and free compound **7a**. $c(\text{DNA}) = 5.20 \times 10^{-5}$ mol/L, and $c(\text{compound } \mathbf{7a}) = 0\text{--}2.0 \times 10^{-5}$ mol/L for curves a–i respectively at increment 0.25×10^{-5} mol/L.

3.6.2 Absorption spectra of NR interaction with DNA

To further understand the interaction between compound **7a** and DNA, the absorption spectra of the competitive interaction of compound **7a** were also investigated. Neutral red (NR) is a planar phenazine dye, which possesses lower toxicity, higher stability and convenient application in comparison with other common probes. It has been sufficiently demonstrated that the binding of NR with DNA is an intercalation binding.²² Therefore, NR was employed as a spectral probe to investigate the binding mode of compound **7a** with DNA in present work. The absorption spectra of the NR dye upon the addition of DNA were shown in Fig. S2 (ESI†). The absorption peak of NR at around 460 nm gradually decreased with the increasing concentration of DNA, and a new band at around 530 nm generated, which could be ascribed to the formation of the new DNA–NR complex. The isosbestic point at 500 nm also provided evidence of DNA–NR complex formation.

3.6.3 Absorption spectra of competitive interaction of compound **7a** and NR with DNA

Figure 6 displayed the absorption spectra of a competitive binding between compound **7a** and NR with DNA. As shown, an apparent intensity increase was observed around 460 nm with the increasing concentration of compound **7a**. In comparison with the absorption around 460 nm of free NR in

the presence of the increasing concentrations of DNA (ESI† Fig. S2), the absorbance at the same wavelength exhibited the reverse process (inset of Fig. 6). The results suggested that compound **7a** could intercalate into the double helix of DNA by substituting NR in the DNA–NR complex.

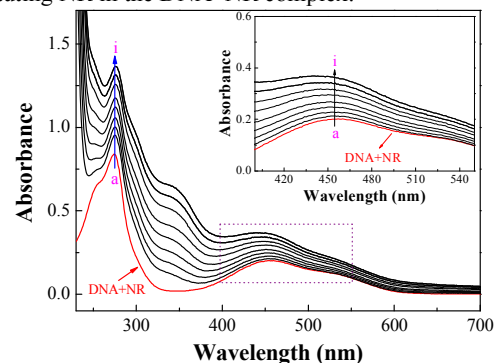


Fig. 6 UV absorption spectra of the competitive reaction between compound **7a** and NR with DNA. $c(\text{DNA}) = 4.20 \times 10^{-5}$ mol/L, $c(\text{NR}) = 2 \times 10^{-5}$ mol/L, and $c(\text{compound } \mathbf{7a}) = 0\text{--}2.0 \times 10^{-5}$ mol/L for curves a–i respectively at increment 0.25×10^{-5} . (Inset) absorption spectra of the system with the increasing concentration of **7a** in the wavelength range of 400–550 nm absorption spectra of competitive reaction between compound **7a** and NR with DNA.

3.7 Cleavage ability towards pUC19 DNA

DNA cleavage is controlled by relaxation of supercoiled form DNA (Form I). Plasmid pUC19 DNA, a widely used DNA cleavage substrate, is acircular double stranded DNA (Form I). The cleavage agent can convert Form I to nicked form (Form II) or linear form DNA (Form III). In gel electrophoresis, the migration rate of the three DNA forms is usually in the order: Form I > Form III > Form II. In order to assess the DNA cleavage activities, the cleavage of plasmid pUC19 DNA assays was investigated by agarose gel electrophoresis. The degradation of plasmid pUC19 DNA from Form I to Form II and Form III in Fig. S3 (ESI†) suggested that compound **7a**– Zn^{2+} complex might cleave DNA effectively at low concentration about 1.25×10^{-5} mol/L, and it must be pointed out that in Fig. S3 (ESI†) berberine, compound **7a** and Zn^{2+} ion could not cleave DNA totally alone. It could be deduced that compound **7a** was able to form complex with Zn^{2+} ion, which might further destroy DNA directly and thus exert its antibacterial activity.²³

3.8 Interactions of compound **7a** with HSA

HSA is an important extracellular protein with extensive distribution in the circulatory system, transports various exogenous and endogenous molecules, thus significantly affecting absorption, distribution, and metabolism of numerous therapeutic drugs.²⁴ Therefore, the molecular characterization of drugs–HSA interaction is not only beneficial to understand pharmacokinetic properties, but also instructive to design new drug molecules.

3.8.1 UV-vis absorption spectral study

UV–vis absorption spectroscopic method is a convenient technique applicable to measure the structural change of protein and to identify complex formation. The UV–vis absorption measurement to study the interaction of compound **7a** with HSA was carried out and the results were shown in Fig. 7. The absorption peak at 278 nm was attributed to the aromatic rings in tryptophan (Trp-214), tyrosine (Tyr-411) and phenylalanine (Phe) residues in HSA. With the

addition of compound **7a**, the peak intensity increased, indicating that compound **7a** could interact with HSA. However, the maximum absorption wavelength remained unchanged, suggesting the interactions of compound **7a** and HSA were noncovalent interactions. These occurred *via* π - π stacking between the aromatic rings of compound **7a** and Trp, Tyr and Phe residues, which possess conjugated π -electrons and are located in the binding cavity of HSA.²⁵

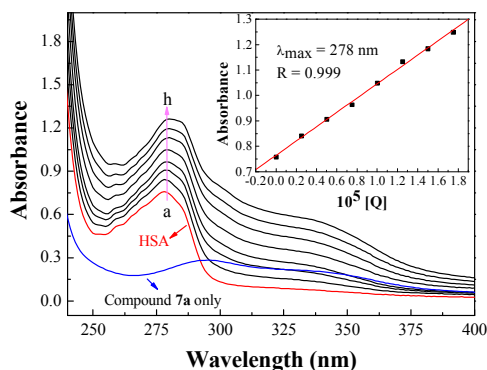


Fig. 7 Effect of compound **7a** to HSA UV-vis absorption, $c(\text{HSA}) = 1.0 \times 10^{-5}$ mol/L; $c(\text{compound } 7a)/(10^{-5} \text{ mol/L})$: 0, 0.25, 0.5, 0.75, 1, 1.25, 1.5, 1.75 ($T = 298 \text{ K}$, $\text{pH} = 7.4$). The inset corresponds to the absorbance at 278 nm with different concentrations of compound **7a**.

3.8.2 Fluorescence quenching mechanism

Fluorescence quenching is considered as an effective approach to investigate the transportation ability of HSA to small molecules. The fluorescence intensity of Trp-214 may change when HSA interacts with other small molecules, which could be reflected in the fluorescence spectra of HSA in the UV region. With a fixed amount of HSA, the fluorescence changes of HSA ($T = 298 \text{ K}$, $\lambda_{\text{ex}} = 295 \text{ nm}$) in the presence of different amounts of compound **7a** were determined. The blue line in Fig. 8 was the only emission spectrum of the active molecule **7a**, which implied that its fluorescence intensity was very weak and could be negligible in comparison with the fluorescence of HSA at the excitation wavelength. The maximum emission peak of HSA at 352 nm in the fluorescence spectra exhibited a progressive decrease in the fluorescence intensity. However, the maximum emission wavelength of HSA remained unchanged, which revealed that Trp-214 did not undergo any change in polarity, and hence compound **7a** was likely to interact with HSA *via* the hydrophobic region located in HSA.

The fluorescence quenching data can be elucidated by the well-known Stern–Volmer equation:

$$\frac{F_0}{F} = 1 + K_{\text{SV}}[Q] = 1 + K_q\tau_0[Q] \quad (2)$$

where F_0 and F are the fluorescence intensities in the absence and presence of compound **7a**, respectively. K_{SV} (L/mol) is the Stern–Volmer quenching constant, $[Q]$ is the concentration of compound **7a**, K_q is the bimolecular quenching rate constant (L mol⁻¹ s⁻¹), τ_0 is the fluorescence lifetime of the fluorophore in the absence of quencher, assumed to be $6.4 \times 10^{-9} \text{ s}$ for HSA. Hence, the Stern–Volmer plots of HSA in the presence of compound **7a** at different concentrations and temperatures could be calculated and were shown in Fig. S4 (ESI†).

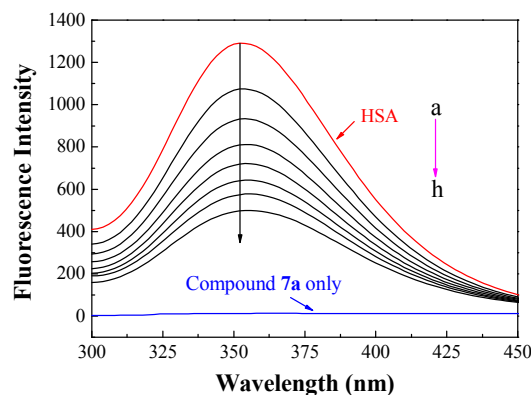


Fig. 8 Emission spectra of HSA with various concentrations of compound **7a**. $c(\text{HSA}) = 1.0 \times 10^{-5}$ mol/L; $c(\text{compound } 7a)/(10^{-5} \text{ mol/L})$, a–h: from 0.0 to 1.17 at increments of 0.167; blue and red lines are the emission spectrum of compound **7a** only and HSA only, respectively; $T = 298 \text{ K}$, $\lambda_{\text{ex}} = 295 \text{ nm}$.

The fluorescence quenching mechanisms are usually classified as either dynamic quenching or static quenching, which could be distinguished by their different dependence on temperature and viscosity. For dynamic quenching, higher temperatures result in faster diffusion and larger amounts of collisional quenching. As a result, the quenching constants are expected to increase with a gradually increasing temperature in dynamic quenching, but the reverse effect would be observed for static quenching. The calculated values of K_{SV} and K_q for the interaction of compound **7a** with HSA at different temperatures were listed in Table S3 (ESI†). The K_{SV} values were inversely correlated with temperature, which indicated that the probable fluorescence quenching of HSA was initiated by the formation of **7a**–HSA complex rather than by dynamic collisions. Furthermore, the obtained larger K_q values (2.55×10^{13} , 2.05×10^{13} and $1.70 \times 10^{13} \text{ L mol}^{-1} \text{ s}^{-1}$ at 288 K, 298 K, 310 K, respectively) were far exceeded the diffusion controlled rate constants of various quenchers with a biopolymer ($2.0 \times 10^{10} \text{ L mol}^{-1} \text{ s}^{-1}$), which suggested that the quenching was not initiated by the dynamic diffusion process but occurred in the static quenching of **7a**–HSA complex.²⁶

The difference in absorption spectroscopy was used to obtain spectra to reconfirm that the probable fluorescence quenching mechanism of HSA by compound **7a** was mainly initiated by ground-state complex formation. The UV-vis absorption spectrum of HSA (ESI† Fig. S5, curve C) and the difference spectrum between HSA–compound **7a** 1:1 complex and compound **7a** (ESI† Fig. S5, curve D) could not be superposed, this result reconfirmed that the probable fluorescence quenching mechanism of HSA by compound **7a** might be a static quenching procedure.²⁷

3.8.3 Binding constant and sites

For a static quenching procedure, quenching data were analyzed according to the modified Stern–Volmer equation:

$$\frac{F_0}{\Delta F} = \frac{1}{f_a K_a [Q]} + \frac{1}{f_a} \quad (3)$$

where ΔF denotes the difference in fluorescence in the absence and presence of compound **7a** at concentration $[Q]$, f_a is the fraction of accessible fluorescence, and K_a is the effective quenching constant for the accessible fluorophores, which are analogous to associative binding constants for the quencher–acceptor system. The dependence

ARTICLE

Journal Name

of $F_0/\Delta F$ on the reciprocal value of quencher concentration $[Q]^{-1}$ is linear with the slope equaling to the value of $(f_a K_a)^{-1}$. The value f_a^{-1} is fixed on the ordinate. The constant K_a is a quotient of the ordinate f_a^{-1} and the slope $(f_a K_a)^{-1}$. The modified Stern–Volmer plots were shown in Fig. S6 (ESI†), and the calculated results were listed in Table S4 (ESI†).

The Scatchard equation could be used to estimate the equilibrium binding constant (K_b) and the number of binding sites (n); it is described as:

$$\log[(F_0/F) - 1] = \log K_b + n \log[Q] \quad (4)$$

Fig. 9 displayed the plots of $\log(F_0 - F)/F$ versus $\log[Q]$ for the interaction between HSA and compound **7a** at various temperatures. K_b and n obtained from the Scatchard plots are listed in Table S4 (ESI†). The decreased trend of K_a and K_b with increased temperatures was in accordance with the temperature dependence of K_{SV} 's. The value of binding site approximates to 1, indicating that only one high affinity binding site was present in the interaction of compound **7a** with HSA. The results also showed that the binding constants were moderate and the effects of temperatures were not obvious, thus compound **7a** might be stored and carried by this protein.

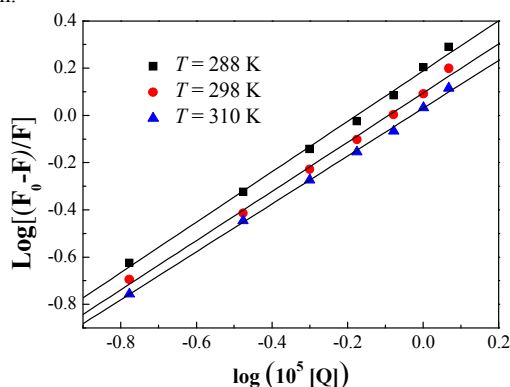


Fig. 9 Scatchard plots of **7a**–HSA system at different temperatures.

3.8.4 Binding mode and thermodynamic parameters

Generally, the major forces involved in small molecules and biomolecules interactions include hydrogen bonds, electrostatic interactions, van der Waals forces, and hydrophobic interactions.²⁸ Thermodynamic parameters like enthalpy change (ΔH) and entropy change (ΔS) of binding reaction are the main evidence for confirming the interactions between small molecules and protein. If ΔH does not vary significantly in the temperature range studied, both its value and ΔS can be estimated from the van't Hoff equation as follows:

$$\ln K = -\frac{\Delta H}{RT} + \frac{\Delta S}{R} \quad (5)$$

where K is analogous to the associative binding constants at the corresponding temperature and R is the gas constant. To elucidate the binding model between compound **7a** and HSA, the thermodynamic parameters were calculated from the van't Hoff plots. The enthalpy change (ΔH) was estimated from the slope of the van't Hoff relationship (ESI† Fig. S7). The free energy change (ΔG) was then calculated from the following equation:

$$\Delta G = \Delta H - T\Delta S \quad (6)$$

Table S5 (ESI†) summarized the values of ΔH , ΔG and ΔS . The negative values of the free energy ΔG of the interactions between compound **7a** and HSA indicated that the binding process was spontaneous. The negative values of ΔH suggested that the binding was predominately enthalpy driven and involved an exothermic reaction. The positive ΔS value is frequently taken as a typical evidence for hydrophobic interaction, which is consistent with the above discussion. The negative ΔH value (-9.498 kJ/mol) observed cannot be mainly attributed to electrostatic interactions since the ΔH values of electrostatic interactions were very small, almost zero. Therefore, $\Delta H < 0$ and $\Delta S > 0$ obtained in this case indicated that both hydrophobic interactions and hydrogen bonds played a major role in the binding of compound **7a** to HSA, and electrostatic interactions might also involve in the binding process.

4. Conclusion

In conclusion, a series of novel Schiff-base bridged THPB triazoles as antimicrobial agents have been successfully developed for the first time by an easy, convenient and economic procedure, and their structures were characterized by HRMS, NMR and IR spectra. The *in vitro* biological evaluation revealed that some of the prepared compounds exerted good to better antibacterial and antifungal activities in comparison with the reference drugs. Noticeably, THPB triazole **7a** could effectively inhibit the growth of *B. yeast*, *M. luteus* and MRSA with MIC values of 0.5, 1 and 2 $\mu\text{g/mL}$, respectively. Further research suggested that compound **7a** could rapidly kill MRSA and induce bacterial resistance more slowly than norfloxacin. Molecular docking indicated that target compound **7a** could bind with MRSA DNA through hydrogen bonds. SARs revealed that the combination of triazole fragment and THPB was beneficial to exert biological activity, and the substituents on the benzyl moiety as well length of alkyl chain at 9-position of THPB influenced the antibacterial potency. The binding investigation of compound **7a** with HSA revealed that this molecule could be effectively transported by HSA. The preliminary exploration for antimicrobial mechanism disclosed that compound **7a** could not only form stable **7a**–DNA complex with calf thymus DNA by an intercalating mode, but also directly cleave pUC19 DNA by formation of complex with Zn^{2+} ion, thus exerting antibacterial activity. Therefore, this work revealed that compound **7a** might be a potentially dual DNA-targeting antibacterial molecule with better water solubility than berberine, which should be a promising start as novel antibacterial agent to overcome drug resistance.

Acknowledgements

This work was partially supported by National Natural Science Foundation of China (Nos. 21672173, 21372186), the Research Fellowship for International Young Scientists from International (Regional) Cooperation and Exchange Program of China National Natural Science Foundation (81650110529), Chongqing Research Program of Basic Research and Frontier Technology (No.cstc2013jcyjA50012, cstc2016jcyjA0508), China Postdoctoral Science Foundation funded project (2014M562326, 2016T90851).

Notes and references

- (a) E. D. Brown and G. D. Wright, *Nature*, 2016, **529**, 336-343; (b) M. Baym, L. K. Stone and R. Kishony, *Science*, 2016, **351**, aad3292; (c) L. Zhang, X. M. Peng, G. L. V. Damu, R. X. Geng and C. H. Zhou, *Med. Res. Rev.*, 2014, **34**, 340-437; (d) X. M. Peng, G. L. V. Damu and C. H. Zhou, *Curr. Pharm. Des.*, 2013, **19**, 3884-3930.
- (a) M. G. Moloney, *Trends Pharmacol. Sci.*, 2016, **37**, 689-701; (b) H. H. Gong, D. Addla, J. S. Lv and C. H. Zhou, *Curr. Top. Med. Chem.*, 2016, **16**, 3303-3364; (c) Y. Cheng, H. Wang, D. Addla and C. H. Zhou, *Chin. J. Org. Chem.*, 2015, **36**, 1-42 (in Chinese); (d) S. C. He, P. Jeyakkumar, S. R. Avula, X. L. Wang, H. Z. Zhang and C. H. Zhou, *Sci. Sinica Chim.*, 2016, **46**, 823-847 (in Chinese).
- L. N. Silva, K. R. Zimmer, A. J. Macedo and D. S. Trentin, *Chem. Rev.*, 2016, **116**, 9162-9236.
- (a) A. R. Ball, G. Casadei, S. Samosorn, J. B. Bremner, F. M. Ausubel, T. I. Moy and K. Lewis, *ACS Chem. Biol.*, 2006, **1**, 594-600; (b) M. Tillhon, L. M. G. Ortiz, P. Lombardi and A. I. Scovassi, *Biochem. Pharmacol.*, 2012, **84**, 1260-1267.
- (a) A. Kumar, Ekavali, K. Chopra, M. Mukherjee, R. Pottabathini and D. K. Dhull, *Eur. J. Pharmacol.*, 2015, **761**, 288-297; (b) S. Preeti, U. Prabhat, M. Shardendu, S. Ananya and P. Suresh, *World J. Pharm. Pharm. Sci.*, 2015, **4**, 547-573.
- (a) M. Ishikawa and Y. Hashimoto, *J. Med. Chem.*, 2011, **54**, 1539-1554; (b) T. Takeuchi, S. Oishi, M. Kaneda, H. Ohno, S. Nakamura, I. Nakanishi, M. Yamane, J. Sawada, A. Asai and N. Fujii, *ACS Med. Chem. Lett.*, 2014, **5**, 566-571.
- (a) J. Mo, Y. Guo, Y. S. Yang, J. S. Shen, G. Z. Jin and X. Zhen, *Curr. Med. Chem.*, 2007, **14**, 2996-3002; (b) H. Y. Chu, G. Z. Jin, E. Friedman and X. C. Zhen, *Cell. Mol. Neurobiol.*, 2008, **28**, 491-499; (c) H. X. Ge, J. Zhang, L. Chen, J. P. Kou and B. Y. Yu, *Bioorg. Med. Chem.*, 2013, **21**, 62-69; (d) D. L. Guo, J. Li, H. Lin, Y. Zhou, Y. Chen, F. Zhao, H. F. Sun, D. Zhang, H. L. Li, B. K. Shoichet, L. Shan, W. D. Zhang, X. Xie, H. L. Jiang and H. Liu, *J. Med. Chem.*, 2016, **59**, 9489-9502.
- P. Cheng, B. Wang, X. B. Liu, W. Liu, W. S. Kang, J. Zhou and J. G. Zeng, *Nat. Prod. Res.*, 2014, **28**, 413-419.
- (a) H. Z. Zhang, L. L. Gan, H. Wang and C. H. Zhou, *Mini-Rev. Med. Chem.*, 2017, **17**, 122-166; (b) X. M. Peng, G. X. Cai and C. H. Zhou, *Curr. Top. Med. Chem.*, 2013, **13**, 1963-2010; (c) H. Z. Zhang, G. L. V. Damu, G. X. Cai and C. H. Zhou, *Curr. Org. Chem.*, 2014, **18**, 359-406; (d) X. J. Fang, P. Jeyakkumar, S. R. Avula, Q. Zhou and C. H. Zhou, *Bioorg. Med. Chem. Lett.*, 2016, **26**, 2584-2588.
- (a) R. Kaur, A. R. Dwivedi, B. Kumar and V. Kumar, *Anti-Cancer Agents Med. Chem.*, 2016, **16**, 465-489; (b) C. H. Zhou and Y. Wang, *Curr. Med. Chem.*, 2012, **19**, 239-280; (c) Y. Wang and C. H. Zhou, *Sci. Sinica Chim.*, 2011, **41**, 1429-1456 (in Chinese).
- (a) D. Allen, D. Wilson, R. Drew and J. Perfect, *Expert Rev. Anti-Infect. Ther.*, 2015, **13**, 787-798; (b) X. F. Cao, Z. S. Sun, Y. B. Cao, R. L. Wang, T. K. Cai, W. J. Chu, W. H. Hu and Y. S. Yang, *J. Med. Chem.*, 2014, **57**, 3687-3706.
- (a) L. Zhang, J. J. Chang, S. L. Zhang, G. L. V. Damu, R. X. Geng and C. H. Zhou, *Bioorg. Med. Chem.*, 2013, **21**, 4158-4169; (b) S. L. Zhang, J. J. Chang, G. L. V. Damu, B. Fang, X. D. Zhou, R. X. Geng and C. H. Zhou, *Bioorg. Med. Chem. Lett.*, 2013, **23**, 1008-1012; (c) S. Q. Wen, P. Jeyakkumar, S. R. Avula, L. Zhang and C. H. Zhou, *Bioorg. Med. Chem. Lett.*, 2016, **26**, 2768-2773.
- (a) Z. Q. Liao, C. Dong, K. E. Carlson, S. Srinivasan, J. C. Nwachukwu, R. W. Chesnut, A. Sharma, K. W. Nettles, J. A. Katzenellenbogen and H. B. Zhou, *J. Med. Chem.*, 2014, **57**, 3532-3545; (b) H. H. Gong, K. Baathulaa, J. S. Lv, G. X. Cai and C. H. Zhou, *Med. Chem. Commun.*, 2016, **7**, 924-931.
- (a) C. Y. Lo, L. C. Hsu, M. S. Chen, Y. J. Lin, L. G. Chen, C. D. Kuo and J. Y. Wu, *Bioorg. Med. Chem. Lett.*, 2013, **23**, 305-309; (b) L. Huang, Z. H. Luo, F. He, A. D. Shi, F. F. Qin and X. S. Li, *Bioorg. Med. Chem. Lett.*, 2010, **20**, 6649-6652.
- P. Jeyakkumar, L. Zhang, S. R. Avula and C. H. Zhou, *Eur. J. Med. Chem.*, 2016, **122**, 205-215.
- C. H. Zhou, P. Jayakumar and X. M. Peng, CN Pat. 2016/105218537, 2016.
- T. Kametani, K. Fukumoto, T. Terui, K. Yamaki and E. Taguchi, *J. Chem. Soc. C*, 1971, 2709-2711.
- (a) J. Hoque, M. M. Konai, S. Gonuguntla, G. B. Manjunath, S. Samaddar, V. Yarlagadda and J. Haldar, *J. Med. Chem.*, 2015, **58**, 5486-5500; (b) Y. Cheng, S. R. Avula, W. W. Gao, D. Addla, V. K. R. Tangadanchu, L. Zhang, J. M. Lin and C. H. Zhou, *Eur. J. Med. Chem.*, 2016, **124**, 935-945.
- L. Zhang, K. V. Kumar, S. Rasheed, R. X. Geng and C. H. Zhou, *Chem. Biol. Drug Des.*, 2015, **86**, 648-655.
- (a) E. J. Denning and A. D. MacKerell Jr, *J. Am. Chem. Soc.*, 2011, **133**, 5770-5772; (b) D. Addla, S. Q. Wen, S. K. Maddili, L. Zhang and C. H. Zhou, *Med. Chem. Commun.*, 2016, **7**, 1988-1994; (c) L. Zhang, K. V. Kumar, S. Rasheed, S. L. Zhang, R. X. Geng and C. H. Zhou, *Med. Chem. Commun.*, 2015, **6**, 1303-1310.
- (a) G. Zhang, P. Fu, L. Wang and M. Hu, *J. Agric. Food Chem.*, 2011, **59**, 8944-8952; (b) X. M. Peng, K. V. Kumar, G. L. Damu and C. H. Zhou, *Sci. Sinica Chim.*, 2016, **59**, 878-894.
- (a) F. Liu, X. L. Wang, X. Han, X. X. Tan and W. J. Kang, *Int. J. Biol. Macromol.*, 2015, **77**, 92-98; (b) L. L. Dai, H. Z. Zhang, S. Nagarajan, S. Rasheed and C. H. Zhou, *Med. Chem. Commun.*, 2015, **6**, 147-154.
- X. M. Peng, L. P. Peng, S. Li, A. S. Rao, K. V. Kumar, S. L. Zhang, K. Y. Tam and C. H. Zhou, *Future Med. Chem.*, 2016, **8**, 1927-1940.
- (a) Y. Guo, F. Yang and H. Liang, *Curr. Top. Med. Chem.*, 2016, **16**, 996-1008; (b) L. P. Peng, S. Nagarajan, S. Rasheed and C. H. Zhou, *Med. Chem. Commun.*, 2015, **6**, 222-229.
- V. D. Suryawanshi, P. V. Anbhule, A. H. Gore, S. R. Patil and G. B. Kolekar, *Ind. Eng. Chem. Res.*, 2012, **51**, 95-102.
- (a) D. P. Yeggoni, A. Rachamallub and R. Subramanyam, *RSC Adv.*, 2016, **6**, 40225-40237; (b) S. L. Zhang, J. J. Chang, G. L. V. Damu, R. X. Geng and C. H. Zhou, *Med. Chem. Commun.*, 2013, **4**, 839-846.
- (a) S. F. Cui, D. Addla and C. H. Zhou, *J. Med. Chem.*, 2016, **59**, 4488-4510; (b) Y. J. Hu, Y. Liu and X. H. Xiao, *Biomacromolecules*, 2009, **10**, 517-521.
- (a) M. T. Rehman, H. Shamsi and A. U. Khan, *Mol. Pharmaceutics*, 2014, **11**, 1785-1797; (b) B. T. Yin, C. Y. Yan, X. M. Peng, S. L. Zhang, S. Rasheed, R. X. Geng and C. H. Zhou, *Eur. J. Med. Chem.*, 2014, **71**, 148-159.

Design, synthesis and biological evaluation of novel Schiff base-bridged tetrahydroprotoberberine triazoles as new type of potential antimicrobial agents

Jun-Rong Duan,^a Han-Bo Liu,^a Ponmani Jeyakkumar,^{§a} Lavanya Gopala,^{#a} Shuo Li,^{*b} Rong-Xia Geng^a and Cheng-He Zhou^{*a}

^a Institute of Bioorganic & Medicinal Chemistry, Key Laboratory of Applied Chemistry of Chongqing Municipality, School of Chemistry and Chemical Engineering, Southwest University, Chongqing 400715, PR China.

^b School of Chemical Engineering, Chongqing University of Technology, Chongqing 400054, PR China.

[§] Ph.D candidate from India.

[#] Postdoctoral fellow from Sri Venkateswara University, Tirupati 517502, India.

Synthesis of a series of Schiff base-bridged tetrahydroprotoberberine triazoles as a new type of potential antimicrobial agents, and preliminary interactions with DNA indicated the possible interaction mechanism.

